

^{203,205}Tl NMR Studies of Crystallographically Characterized Thallium Alkoxides. X-ray Structures of [Ti(OCH₂CMe₃)₄ and [Ti(OAr)]_∞, Where OAr = OC₆H₃(Me)_{2-2,6} and OC₆H₃(CHMe₂)_{2-2,6}

Cecilia A. Zechmann, Timothy J. Boyle,* and Dawn M. Pedrotty

Sandia National Laboratories, Advanced Materials Laboratory, 1001 University Boulevard, SE, Albuquerque, New Mexico 87106

Todd M. Alam and David P. Lang

Sandia National Laboratories, Department of Organic Materials, P.O. Box 5800, Albuquerque, New Mexico, 87185-1407

Brian L. Scott

Los Alamos National Laboratories, CST-18, Chemical Science and Technology Division, X-ray Diffraction Laboratory, Los Alamos, New Mexico 87545

Received June 8, 2000

[Ti(OCH₂Me)₄ (**1**) was reacted with excess HOR to prepare a series of [Ti(OR)]_n, where OR = OCHMe₂ (**2**, *n* = 4), OCM₂Me₃ (**3**, *n* = 4), OCH₂CMe₃ (**4**, *n* = 4), OC₆H₃(Me)_{2-2,6} (**5**, *n* = ∞), and OC₆H₃(CHMe₂)_{2-2,6} (**6**, *n* = ∞). Single-crystal X-ray diffraction experiments revealed that in the solid state the alkoxide-ligated compound **4** adopts a cubane structure, whereas the aryloxide derivatives, **5** and **6**, formed polymeric chains. Compounds **1–6** were also characterized by ^{203,205}Tl solution and ²⁰⁵Tl solid-state NMR spectroscopy. In solution it was determined that **1–4** retained the [Ti–O]₄ cube structure, whereas the polymeric species **5** and **6** appeared to be fluxional. Variations in the solution and solid-state structures for the [Ti(OR)]₄ cubes and polymeric [Ti(OAr)]_∞ are influenced by the steric hindrance of the ligand. The acidity of the parent alcohol influences the degree of covalency at the Tl metal center, which is reflected in the ^{203,205}Tl chemical shifts for **1–6**.

Introduction

Metal alkoxides have been found to be excellent precursors for the production of ceramic oxide materials.^{1–5} “Single-source” precursors (heterometallic alkoxides) are of interest for the production of complex ceramics because they may reduce the processing time and crystallization temperature of the final materials and increase control over the final cation stoichiometry. Many synthetic routes have been utilized in an attempt to generate heteronuclear metal alkoxides with varied levels of success. For instance, simple mixing of metal alkoxides often results in a homogeneous solution but does not always yield heteronuclear precursors upon crystallization.^{6–8} Alternatively, metathesis reactions, which refers to the introduction of a metal cation that can be easily exchanged for another metal, can also

be used for the production of mixed-metal species.^{1–5} However, this approach often yields products that include spurious atoms. For example, alkali metal alkoxides (AOR = LiOR, NaOR, KOR) have been shown to be acceptable for the first step—introduction of a metathesizable cation.^{1–4,9,10} In the titanium system, the parent alkoxide (Ti(OR)₄) reacts with AOR to easily generate (eq 1) the heterometallic species [ATi(OR)₅]_n (*n* = 2 or ∞, depending upon the OR ligand).^{9–12} But when these double



alkoxides are then used to produce more complex species (eq 2),^{9–12} the “Ti(OR)₅” anion does not always cleanly transfer, resulting in halide or alkali metal retention.^{9,10} To understand this phenomenon, we investigated the solid-state structures of the [ATi(OR)₅]_n and found that the arrangement of the cations limits the accessibility of the alkali metal cation.^{9,10}

* To whom correspondences should be addressed.

- (1) Caulton, K. G.; Hubert-Pfalzgraf, L. G. *Chem. Rev.* **1990**, *90*, 969.
- (2) Bradley, D. C. *Chem. Rev.* **1989**, *89*, 1317.
- (3) Chandler, C. D.; Roger, C.; Hampden-Smith, M. J. *Chem. Rev.* **1993**, *93*, 1205.
- (4) Bradley, D. C.; Mehrotra, R. C.; Gaur, D. P. *Metal Alkoxides*; Academic Press: New York, 1978.
- (5) Veith, M.; Mathur, S.; Mathur, C. *Polyhedron* **1998**, *17*, 1005.
- (6) Mehrotra, R. C.; Agrawal, M. M. *J. Chem. Soc. A* **1967**, 1026.
- (7) Mehrotra, R. C.; Agrawal, M. M.; Kapoor, P. N. *J. Chem. Soc. A* **1968**, 2673.
- (8) Zechmann, C. A.; Huffman, J. C.; Folting, K.; Caulton, K. G. *Inorg. Chem.* **1998**, *37*, 5856.

- (9) Boyle, T. J.; Bradley, D. C.; Hampden-Smith, M. J.; Patel, A.; Ziller, J. W. *Inorg. Chem.* **1995**, *34*, 5893.
- (10) Boyle, T. J.; Alam, T. M.; Tafoya, C. J.; Mechenbier, E. R.; Ziller, J. W. *Inorg. Chem.* **1999**, *38*, 2422.
- (11) Hampden-Smith, M. J.; Williams, D. S.; Rheingold, A. L. *Inorg. Chem.* **1990**, *29*, 4076.
- (12) Mehrotra, R. C. *J. Chem. Soc. A* **1967**, 1026.

In an effort to circumvent some of the problems associated with the generation of multimetal alkoxide compounds using AOR, we chose to investigate an alternative cation for metathesis. Thallium alkoxides ($[\text{Tl}(\text{OR})_n]_n$) were selected because Tl-containing species in other systems have been shown to readily undergo metathesis reactions.^{13,14} Since $[\text{Tl}(\text{OR})_n]$ have been known since the early 1800s (first prepared by Lamy¹⁵), it is surprising that only a few reports exist in the literature that utilize these compounds to generate heteronuclear alkoxide compounds.^{14,16,17} Along with the often reported high toxicity of this metal,¹³ the lack of structural information concerning these species may have prevented further development of $[\text{Tl}(\text{OR})_n]$ in this type of methodology.

From spectroscopic methods and a partial crystal structure of the OMe derivative, preliminary structural information suggests that $[\text{Tl}(\text{OR})_4]$ (OR = OMe, OCH₂Me, OCHMe₂, and OCM₂) compounds adopt cubic geometries;^{18,19} however, none of these alkoxides could be fully characterized by single-crystal X-ray crystallographic methods.¹⁴ It is important to note that an abundance (>50) of Tl(I)-containing species have been crystallographically characterized,²⁰ including a number of cyclopentadienyl derivatives ($[\text{Tl}(\text{Cp})_\infty]$).^{21–29} From the Tl(I) family of crystallographically characterized compounds, only two aryloxide derivatives have been structurally identified, $[\text{Tl}\{\mu\text{-O}(\text{C}_6\text{H}_4)(\text{C}_6\text{H}_4\text{OH})\}_2]$ ³⁰ and $[\text{Tl}(\text{OC}_6\text{H}_2\text{-2,4,6-(CF}_3)_3)_2]$.³¹ Since it is important to know the structure of $[\text{Tl}(\text{OR})_n]$ in order to exploit them synthetically, we initiated a study of these compounds, including OR = OCH₂Me (**1**, $n = 4$),^{18,19} OCHMe₂ (**2**, $n = 4$),^{18,19} OCM₂ (**3**, $n = 4$),^{18,19} OCH₂CM₂ (**4**, $n = 4$), OC₆H₃(Me)₂-2,6 (DMP, **5**, $n = \infty$), and OC₆H₃(CHMe₂)₂-2,6 (DIP, **6**, $n = \infty$), using ¹H, ¹³C, and ^{203,205}Tl NMR spectroscopy, and X-ray crystallography when possible. Details of the synthesis and characterization of these compounds are discussed below.

Experimental Section

All compounds described below were handled with rigorous exclusion of air and water using standard Schlenk line and glovebox techniques. FT-IR data was obtained on a Bruker Vector 22 using KBr

pellets under an atmosphere of flowing nitrogen. TGA/DTA experiments were performed on a Polymer Laboratories STA 1500 instrument under an atmosphere of flowing oxygen up to 650 °C at a ramp rate of 5 °C/min. Elemental analyses were performed on a Perkin-Elmer 2400 CHN–S/O elemental analyzer.

For the solid-state NMR investigations, each sample was prepared from dried crystalline material that was handled and stored under an argon atmosphere. A standard single-pulse Bloch decay, 64–128 scan averages, 2 s recycle delay, and a 2 μs pulse were used for all experiments. The ²⁰⁵Tl spectra were referenced to solid Tl(NO₃) ($\delta = 0.0$ ppm).

For solution spectra, each dried crystalline sample was redissolved in an appropriate deuterated solvent at saturated solution concentrations and sealed under vacuum. All solution spectra were obtained on a DMX400 spectrometer at 399.9 and 100.5 MHz for ¹H and ¹³C{¹H} experiments, respectively. A 5 mm bb probe was used for all experiments. ¹H NMR spectra were obtained using a direct single-pulse excitation with a 10 s recycle delay. ¹³C{¹H} NMR spectra were obtained using composite pulse ¹H decoupling with a 5 s recycle delay and a $\pi/4$ pulse excitation. High-resolution solution ^{203,205}Tl NMR spectra were obtained on a Bruker DMX400 at 231.0 and 228.9 MHz for ²⁰⁵Tl and ²⁰³Tl, respectively. All spectra were obtained on a specially tuned 5 mm Tl{¹H} probe, using single-pulse excitation and a 1 s recycle delay. Both the ²⁰³Tl and ²⁰⁵Tl spectra were referenced to 0.001 M Tl(NO₃) in D₂O ($\delta = 0.0$ ppm). Simulations of the multiplet patterns in the ^{203,205}Tl high-resolution spectra were obtained using the simulation component in the NMR Utility Transform Software (NUTS) program (Acorn NMR, Fremont, CA). The simulation program was modified to include both the ²⁰⁵Tl and ²⁰³Tl spin $1/2$ nuclei along with the relative natural abundance of these two nuclei, 70.5% and 29.5%, respectively.

Isopropanol (HOCHMe₂) and all solvents were freshly distilled from the appropriate drying agent³² and stored over molecular sieves. 3-Butanol (HOCMe₃) was dissolved in hexanes (1.7 M solution) and stored over molecular sieves for a minimum of 24 h prior to use. The following compounds were stored under argon upon receipt (Aldrich) and used without further purification: neopentanol (HOCH₂CM₂), 2,6-dimethylphenol (H-DMP), 2,6-diisopropylphenol (H-DIP), and $[\text{Tl}(\text{OCH}_2\text{Me})_4]$, **1**. Since **2–6** were all prepared in a similar manner, a general synthetic route is described below with any variations noted in the individual sections.

General Synthesis. Compound **1** was added to a solution consisting of a large excess of the appropriate alcohol (HOR) dissolved in toluene. The resulting mixture was stirred overnight at room temperature, followed by warming in a water bath (~50 °C) for 2 h. The solvent was then removed in vacuo, with heating, to facilitate the removal of any remaining volatile material. The resulting solid was redissolved in hexanes (**2–4**), toluene (**5**), or THF (**6**). Any insoluble material was removed by centrifugation, and the final product was isolated by removal of the solvent in vacuo. Crystalline products were isolated by either slow evaporation of solvent or slow cooling of a hot saturated solution.

$[\text{Tl}(\text{OCHMe}_2)_4]$ (**2**). HOCHMe₂ (10 mL, 130 mmol) in toluene (10 mL) and **1** (1.0 mL, 3.5 mmol) in toluene (5 mL) were used. Isolated yield: 2.9 g (78%). FT-IR (KBr, cm⁻¹): 2947(s), 2913(m), 2852(w), 2803(w), 2779(w), 2765(w), 2750(w), 2598(w), 2588(w), 1450(m), 1368(m), 1355(m), 1327(m), 1156(w), 1114(s), 948(s), 810(m), 511(m), 466(m). ¹H NMR (399.9 MHz, C₆D₆, 20 °C): δ 5.16 (1H, sept, OCH(CH₃)₂, ³J_{H–H} = 6 Hz), 1.33 (6H, d, OCH(CH₃)₂, ³J_{H–H} = 6 Hz). ¹³C{¹H} NMR (100.1 MHz, toluene-*d*₈): δ 66.2 (OCH(CH₃)₂), 29.1 (OCH(CH₃)₂). ²⁰⁵Tl NMR (231.0 MHz, toluene-*d*₈): δ 3067 (sept, ²J_{205–203} = 2.57 kHz). ²⁰³Tl NMR (228.9 MHz, toluene-*d*₈): δ 3067 (sept, ²J_{205–203} = 2.57 kHz). TGA (oxygen) (total wt loss (%)) found (calcd for Tl₂O₃): 11.5 (10.0). DTA: exotherm at 210 °C. Anal. Calcd for C₃H₇O₃: C, 13.68; H, 2.68. Found: C, 12.98; H, 2.53.

$[\text{Tl}(\text{OCMe}_3)_4]$ (**3**). HOCMe₃ (10 mL, 105 mmol) in toluene (5 mL) and **1** (0.58 mL, 2.1 mmol) in toluene (5 mL) were used. Yield: 2.02 g (89%). FT-IR (KBr, cm⁻¹): 2948(s), 2916(m), 2886(m), 2853(m), 1456(m), 1376(s), 1353(s), 1215(m), 1173(s), 915(s), 745(m), 499(s),

- (13) Cotton, F. A.; Wilkinson, G. *Advanced Inorganic Chemistry*, 5th ed.; John Wiley & Sons: New York, 1988.
- (14) Janiak, C. *Coord. Chem. Rev.* **1997**, *163*, 107.
- (15) Lamy, A. *Ann. Chim. Phys.* **1863**, *67*, 365.
- (16) Gulliver, E. A.; Garvey, J. W.; Wark, T. A.; Hampden-Smith, M. J.; Datye, A. *J. Am. Ceram. Soc.* **1991**, *74*, 1091.
- (17) Veith, M.; Kunze, K. *Angew. Chem., Int. Ed. Engl.* **1991**, *30*, 95.
- (18) Burke, P. J.; Matthews, R. W.; Gillies, D. G. *J. Chem. Soc., Dalton Trans.* **1980**, 1439.
- (19) Maroni, V. A.; Spiro, T. G. *Inorg. Chem.* **1968**, *7*.
- (20) The Cambridge Database has over 100 structures containing Tl cations. More than 50 of these compounds contain a Tl(I) cation.
- (21) Bruce, M. I.; Walton, J. K.; Williams, M. L.; Hall, S. R.; Skelton, B. W.; White, A. H. *J. Chem. Soc., Dalton Trans.* **1982**, 2209.
- (22) Bakar, W. A. W. A.; Davidson, J. L.; Lindsell, W. E.; McCullough, K. J.; Muir, K. W. *J. Organomet. Chem.* **1987**, *322*, C1.
- (23) Bakar, W. A. W. A.; Davidson, J. L.; Lindsell, W. E.; McCullough, K. J.; Muir, K. W. *J. Chem. Soc., Dalton Trans.* **1989**, 991.
- (24) Klauk, A.; Seppelt, K. *Angew. Chem., Int. Ed. Engl.* **1994**, *33*, 1994.
- (25) Dashti-Mommertz, A.; Neumuller, B.; Melle, S.; Haase, D.; Uhl, W. *Z. Anorg. Allg. Chem.* **1999**, *625*, 1828.
- (26) Drexler, H.-J. Ph.D. Thesis, University of Rostock, Rostock, Germany, 1997.
- (27) Freeman, M. B.; Sneddon, L. G.; Huffman, J. C. *J. Am. Chem. Soc.* **1977**, *99*, 5194.
- (28) Frasson, E.; Menegus, F.; Panattoni, C. *Nature* **1963**, *199*, 1087.
- (29) Werner, H.; Otto, H.; Kraus, H. *J. Organomet. Chem.* **1986**, *315*, C57.
- (30) Elhadad, A. A.; Kickham, J. E.; Loeb, S. J.; Taricani, L.; Tuck, D. G. *Inorg. Chem.* **1995**, *34*, 120.
- (31) Roesky, H. W.; Scholz, M.; Noltemeyer, M.; Edelmann, F. T. *Inorg. Chem.* **1989**, *28*, 3829.

- (32) Perrin, D. D.; Armarego, W. L. F. *Purification of Laboratory Chemicals*, 3rd ed.; Pergamon Press: New York, 1988.

440(w). ^1H NMR (399.9 MHz, toluene- d_8): 1.41 ppm (s, $\text{OC}(\text{CH}_3)_3$). $^{13}\text{C}\{^1\text{H}\}$ NMR (100.1 MHz, toluene- d_8): δ 71.7 ($\text{OC}(\text{CH}_3)_3$), 33.6 ($\text{OC}(\text{CH}_3)_3$). ^{205}Tl NMR (231.0 MHz, toluene- d_8): δ 3285 (sept, $^2J_{205-203} = 2.25$ kHz). ^{203}Tl NMR (228.9 MHz, toluene- d_8): δ 3285 (sept, $^2J_{205-203} = 2.25$ kHz). TGA (oxygen) (total wt loss (%) found (calcd for Tl_2O_3): 16.3 (17.7). DTA: small exotherms at 241 and 272 °C. Anal. Calcd for $\text{C}_4\text{H}_{11}\text{OTl}$: C, 17.19; H, 3.97. Found: C, 16.31; H, 2.92.

[Ti(OCH₂CMe₃)₄ (4). HOCH₂CMe₃ (2.6 g, 29 mmol) in toluene (10 mL) and **1** (0.5 mL, 1.8 mmol) were used. Isolated yield: 1.9 g (92%). X-ray quality crystals could be obtained by slow evaporation (room-temperature) of a saturated hexanes or toluene solution. FT-IR (KBr, cm^{-1}): 2947(s), 2893(m), 2858(m), 2793(m), 2771(m), 2737(w), 2684(m), 1473(m), 1393(m), 1357(m), 1250(w), 1210(w), 1044(s), 1010(s), 930(w), 892(w), 544(m), 415(w). ^1H NMR (399.9 MHz, toluene- d_8): δ 3.61 (2H, s, OCH_2CMe_3), 1.00 (9H, s, OCH_2CMe_3). $^{13}\text{C}\{^1\text{H}\}$ NMR (100.1 MHz, toluene- d_8): δ 76.9 (OCH_2CMe_3), 33.8 (OCH_2CMe_3), 27.3 (OCH_2CMe_3). ^{205}Tl NMR (231.0 MHz, toluene- d_8): δ 2561 (sept, $^2J_{205-203} = 2.58$ kHz). ^{203}Tl NMR (228.9 MHz, toluene- d_8): δ 2562 (sept, $^2J_{205-203} = 2.58$ kHz). TGA (oxygen) (total wt loss (%) found (calcd for Tl_2O_3): 21.0 (21.7). DTA: large exotherm at 205 °C. Anal. Calcd for $\text{C}_{20}\text{H}_{44}\text{O}_4\text{Tl}_4$: C, 20.60; H, 3.80. Found: C, 20.52; H, 3.63.

[Ti(DMP)]_∞ (5). H-DMP (1.24 g, 10.6 mmol) in toluene (12 mL) and **1** (0.70 mL, 2.7 mmol) were used. Crystalline yield: 2.88 g (89%). X-ray quality crystals were obtained upon the cooling of saturated hot toluene or THF solutions. FT-IR (KBr, cm^{-1}): 2998(w), 2961(m), 2922(m), 2906(m), 2840(w), 1581(s), 1457(s), 1410(s), 1367(m), 1318(w), 1262(s), 1231(s), 1158(w), 1086(s), 978(w), 946(w), 910(w), 838(s), 761(s), 681(m), 501(m). ^1H NMR (399.9 MHz, toluene- d_8): δ 7.16 (2H, d, $\text{OC}_6\text{H}_3(\text{CH}_3)_2$, $^3J_{\text{H-H}} = 7.2$ Hz), 6.63 (1H, t, $\text{OC}_6\text{H}_3(\text{CH}_3)_2$, $^3J_{\text{H-H}} = 7.2$ Hz), 2.48 (6H, s, $\text{OC}_6\text{H}_3(\text{CH}_3)_2$). $^{13}\text{C}\{^1\text{H}\}$ NMR (100.1 MHz, toluene- d_8): δ 128.8, 128.3, 127.9, 125.0 ($\text{OC}_6\text{H}_3(\text{CH}_3)_2$), 16.9 ($\text{OC}_6\text{H}_3(\text{CH}_3)_2$). ^{205}Tl NMR (231.0 MHz, toluene- d_8): δ 1989 (s). ^{203}Tl NMR (228.9 MHz, toluene- d_8): δ 1989 (s). TGA (oxygen) (total wt loss (%) found (calcd for Tl_2O_3): 29.9 (32.5). DTA: large exotherm at 391 °C. Anal. Calcd for $\text{C}_8\text{H}_9\text{OTl}$: C, 29.52; H, 2.79. Found: C, 30.03; H, 3.06.

[Ti(DIP)]_∞ (6). H-DIP (3.00 g, 16.8 mmol) in THF (100 mL) and **1** (0.95 mL, 3.4 mmol) were used. Crystalline yield: 3.66 g (71%). X-ray quality crystals were obtained by the slow cooling of hot, saturated THF or pyridine solutions. FT-IR (KBr, cm^{-1}): 2952(s), 2919(m), 2863(m), 1581(m), 1457(m), 1418(s), 1356(m), 1324(s), 1253(s), 1200(m), 1156(m), 1096(m), 1037(w), 883(w), 833(s), 797(w), 762(s), 676(m), 524(m), 446(w), 421(w). ^1H NMR (399.9 MHz, THF- d_8): δ 6.94 (2H, d, $\text{OC}_6\text{H}_3(\text{CH}(\text{Me})_2)_2$, $^3J_{\text{H-H}} = 7.6$ MHz), 6.42 (1H, t, $\text{OC}_6\text{H}_3(\text{CH}(\text{Me})_2)_2$, $^3J_{\text{H-H}} = 7.6$ MHz), 3.87 (2H, sept, $\text{OC}_6\text{H}_3(\text{CH}(\text{CH}_3)_2)_2$, $^3J_{\text{H-H}} = 6.8$ MHz), 1.04 (12H, d, $\text{OC}_6\text{H}_3(\text{CH}(\text{CH}_3)_2)_2$, $^3J_{\text{H-H}} = 6.8$ MHz). $^{13}\text{C}\{^1\text{H}\}$ NMR (100.1 MHz, THF- d_8): δ 159.1, 138.3, 123.1, 116.8 ($\text{OC}_6\text{H}_3(\text{CH}(\text{CH}_3)_2)_2$), 27.4 ($\text{OC}_6\text{H}_3(\text{CH}(\text{CH}_3)_2)_2$), 26.1 ($\text{OC}_6\text{H}_3(\text{CH}(\text{CH}_3)_2)_2$). ^{205}Tl NMR (231.0 MHz, THF- d_8): δ 1840 (s). ^{203}Tl NMR (228.9 MHz, d_8 -THF): δ 1840 ppm (s). TGA (oxygen) (total wt loss (%) found (calcd for Tl_2O_3): 43.7 (40.2). DTA: large exotherm at 412 °C (recoalescence peak). Anal. Calcd for $\text{C}_{24}\text{H}_{34}\text{OTl}$: C, 37.77; H, 4.49. Found: C, 37.83; H, 4.48.

Structure Determinations. For each sample, a suitable crystal was mounted from a pool of Fluorolube HO-125 onto a thin glass fiber and then immediately placed under a liquid N_2 stream on a Bruker AXS diffractometer. Data collection parameters for all compounds are given in Table 1. The radiation used was graphite monochromatized Mo $K\alpha$ radiation ($\lambda = 0.71073$ Å). Lattice determination and data collection were carried out using SMART, version 5.054, software.³³ Data reduction was performed using SAINT+, version 5.02, software.³³ Absorption correction using SADABS³³ in SHELXTL, version 5.1,³³ was carried out for all compounds. Structure solution, graphics, and preparation of publication materials were performed using SHELXTL.³³ After all non-hydrogen atoms were identified, the hydrogen atoms were

Table 1. Data Collection Parameters for **4–6**

	4	5	6
chemical formula	$\text{C}_{20}\text{H}_{44}\text{O}_4\text{Tl}_4$	$\text{C}_8\text{H}_9\text{OTl}$	$\text{C}_{12}\text{H}_{17}\text{OTl}$
fw	1166.03	325.52	381.648
temp (K)	168	168	168
space group	cubic	hexagonal	monoclinic
cryst syst	$P43n$	$R3c$	$P2_1/c$
<i>a</i> (Å)	18.139(1)	25.269(2)	9.510(2)
<i>b</i> (Å)		25.269(2)	6.600(1)
<i>c</i> (Å)		6.632(1)	20.268(4)
β (deg)			102.591(2)
<i>V</i> (Å ³)	5968.2	3667.1	1241.5
<i>Z</i>	8	18	4
<i>D</i> _{calcd} (mg/m ³)	2.595	2.653	
μ (mm ⁻¹)	21.55	19.80	25.952
R1 ^a (%)	6.82	2.21	6.84
wR2 ^b (%) [<i>I</i> > 2 σ (<i>I</i>)]	20.15	5.14	18.88
R1 ^a (% , all data)	10.49	2.35	8.08
wR2 ^b (% , all data)	22.15	5.20	20.15

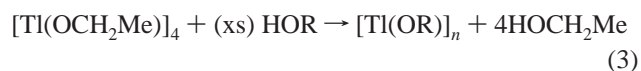
$$^a \text{R1} = \sum ||F_o| - |F_c|| / \sum |F_o|. \quad ^b \text{wR2} = [\sum [w(F_o^2 - F_c^2)^2] / \sum [w(F_o^2)^2]]^{1/2}.$$

fixed in positions of ideal geometry and the entire structure refined within the XShell software.³³ These idealized hydrogen atoms had their isotropic temperature factors fixed at 1.2 or 1.5 times the equivalent isotropic U of the C atoms to which they were bonded. Individual differences in data collection, structure solution, and refinement are reported below.

The systematic absences observed for **4** were consistent with both the centric space group $PM\bar{3}n$ and the acentric space group $P43n$. Attempts to solve the structure in the centric space group were unsuccessful. LePage's symmetry-checking program, run on a $P43n$ structure did not show any additional symmetry. Therefore, the structure of **4** was solved in space group $P43n$ using direct methods and difference Fourier techniques. The initial solution revealed the Tl and O atom positions. There were two independent molecules per unit cell with one molecule on a site of 23 symmetry and the other on a site of -4 symmetry. In the former molecule, the OCH_2CMe_3 group was disordered on a site of 3-fold rotation symmetry. The OCH_2CMe_3 group of the molecule occupying the -4 symmetry element was also severely disordered. Both of these OCH_2CMe_3 groups were modeled as rigid bodies. The modeling of the OCH_2CMe_3 groups in this fashion resulted in a drop of about 3% in R1. While there were still several large temperature factors on some carbon atoms, additional attempts to model the disorder were not successful. The temperature factors are outside the normal range; however, these molecules are occupying sites of very high symmetry (*T* and *S*₄). The molecules themselves do not possess this high symmetry and are therefore disordered to achieve the apparent crystallographic symmetry. The large temperature factors are an artifact of this disorder. Because of the disorder of the OCH_2CMe_3 groups, hydrogen atom positions were not considered in the model. The final refinement converged to R1 = 0.0682 and wR2 = 0.2015, with isotropic temperature factors on all atoms except thallium. Structure solutions and refinements of **5** and **6** were straightforward. Additional details of data collection and structure refinement are listed in Table 1.

Results and Discussion

Synthesis. The $[\text{Ti}(\text{OR})_n]$ investigated in this report were synthesized through an alcohol (HOR) exchange reaction between **1** and the appropriate HOR (eq 3). The complete



exchange of OCH_2Me by OR was ensured through the addition of an excess of HOR and heating of the reaction mixture.

The evolved HOCH_2Me and any excess HOR were removed in vacuo, assisted with mild heating or by filtration, yielding an off-white solid. For **2** and **3**, a small amount of decomposition (formation of a black powder thought to be Tl^0) was noted upon

(33) The listed versions of SAINT, SMART, XShell, and SADABS Software from Bruker Analytical X-Ray Systems, Inc., 6300 Enterprise Lane, Madison, WI 53719 were used in analysis.

Table 2. Selected Distances and Angles for 4–6

4		5		6	
Distances (Å)					
Ti···Ti					
Ti(1A)···Ti(1B)	3.766(3)	Ti(1A)···Ti(1B)	4.516(3)	Ti(1A)···Ti(1B)	4.513(5)
Ti(1A)···Ti(1C)	3.750(2)				
Ti(1A)···Ti(1D)	3.750(2)				
Ti–μ-O					
Ti(1A)–O(1A)	2.463(15)	Ti(1A)–O(1A)	2.589(4)	Ti(1A)–O(1A)	2.588(7)
Ti(1A)–O(1AA)	2.464(17)	Ti(1A)–O(1AA)	2.372(4)	Ti(1A)–O(1AA)	2.429(7)
Ti(1A)–O(1BA)	2.475(17)				
Angles (deg)					
Ti–O–Ti					
Ti(1A)–O(1A)–Ti(1B)	99.7(6)	Ti(1A)–O(1)–Ti(1B)	131.09(18)	Ti(1A)–O(1AA)–Ti(1B)	128.1(3)
Ti(1A)–O(1A)–Ti(1D)	98.8(6)				
Ti(1B)–O(1A)–Ti(1D)	98.8(6)				
O–Ti–O					
O(1A)–Ti(1A)–O(1AA)	79.7(6)	O(1A)–Ti(1A)–O(1AA)	92.16(8)	O(1A)–Ti(1A)–O(1AA)	92.83(13)
O(1A)–Ti(1A)–O(1BA)	80.3(6)				
O(1AA)–Ti(1A)–O(1BA)	80.3(6)				
Ti–O–C					
Ti(1A)–O(1)–C(1)	103.5(15)	Ti(1A)–O(1A)–C(1A)	103.8(4)	Ti(1B)–O(1AA)–C(1AA)	106.6(5)
Ti(1B)–O(1)–C(1)	150.5(9)	Ti(1A)–O(1AA)–C(1AA)	125.0(4)	Ti(1A)–O(1AA)–C(1AA)	124.6(6)
Ti(1D)–O(1)–C(1)	95.5(13)				

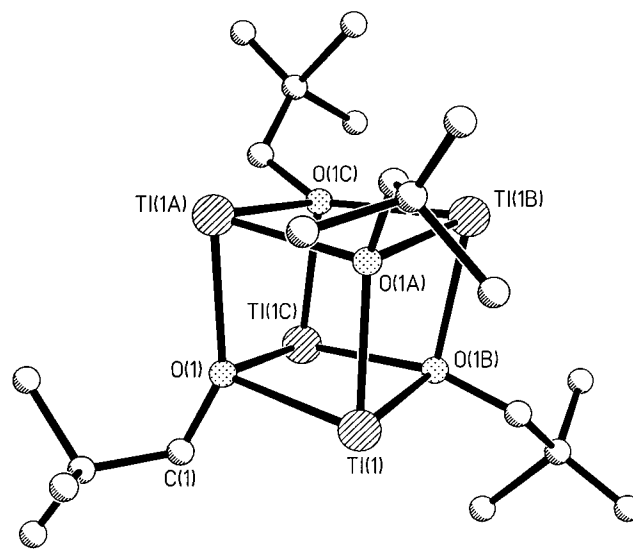
warming. This decomposition was also observed by Sidgwick and Sutton for $[\text{Ti}(\text{OR})_4]$ (OR = OMe, OCH_2Me).³⁴ In each case, the stability of these complexes was greatly enhanced when stored in the parent alcohol.³⁴ Compounds 4–6 demonstrated increased stability in comparison to the smaller alkoxides, and no black precipitate was observed during the synthesis or drying of these compounds. The IR stretches associated with the individual ligands were present in each sample with the expected loss of the O–H stretch (typically observed as a broad resonance at greater than 3000 cm^{-1}). The asymmetric Ti–(μ_3 -O) stretches of 2–4 were observed in the FT-IR at frequencies of $\leq 500\text{ cm}^{-1}$. The Ti–(μ -O) stretch of 5 and 6 were identified at 501 and 524 cm^{-1} , respectively.

During the course of this investigation, it was observed that as the steric bulk of the ligand increased, the solubility of the corresponding $[\text{Ti}(\text{OR})_n]$ decreased (solubility of $1 > 2 > 3 \sim 4 > 5 > 6$). Compounds 1–4 were found to be soluble in hexanes, approaching approximate molarities of miscible, 3.0, 0.30, and 0.30, respectively. Compound 5 was only slightly soluble in toluene, whereas 6 was found to be insoluble in toluene and only slightly soluble in THF. Although steric factors often play a role in determining the solubility of $\text{M}(\text{OR})_x$, the trend is generally the reverse of what was observed for this series of compounds (i.e., typically, the more sterically demanding ligands yield smaller, more soluble compounds). In a previous study, Lee reported that a small decrease in the $\text{p}K_a$ of the aryl alcohol resulted in an increase in the ionic character of the corresponding $[\text{Ti}(\text{OAr})_n]$.³⁵ Since an increase in ionic character typically results in a decrease in solubility in nonpolar solvents, this explanation was invoked to explain the solubility trend observed for 1–6. Crystal structure determinations and solution data were collected on 1–6 to explore this phenomenon.

Solid-State Structures. Table 1 summarizes the collection parameters for 4–6. Table 2 lists selected bond distances and angles for 4–6. Because of the similarities of the two independent $[\text{Ti}(\text{OCH}_2\text{CMe}_3)_4]$ molecules in the unit cell of 4, only one set of metrical data is presented in Table 2. Full structural details are available in Supporting Information.

Several attempts to structurally characterize 2 and 3 were attempted; however, disorder in the crystals did not allow for the connectivity of the final complex to be unambiguously identified. X-ray quality crystals of 4–6 were isolated by slow evaporation or cooling of a hot, saturated solution. Figures 1–3 show the thermal ellipsoid or ball-and-stick plots for 4–6, respectively. Elemental analyses of the bulk powders of 4–6 were consistent with the calculated values; however, the data obtained for 2 and 3 were not acceptable. The deviations are most likely a reflection of the thermal sensitivity of these compounds [noted in the preparation of these compounds (vide infra)],³⁴ which prohibits meaningful thermal elemental analyses.

Several $[\text{Ti}(\text{OR})_n]$ have been characterized by a host of analytical methods as tetrameric cubane compounds.¹⁴ However, only a partial structure of the methoxide derivative, $[\text{Ti}(\text{OMe})_4]$, has been crystallographically determined.³⁶ Because of technical limitations, only the Ti atom positions were refined in this study and the sole metrical data reported for $[\text{Ti}(\text{OMe})_4]$ were Ti···Ti distances. Therefore, the structure of 4 is the first fully refined $[\text{Ti}–\text{O}]_4$ cubane cage. Two independent molecules were identified in the unit cell with significant disorder noted for the

**Figure 1.** Ball and stick plot of 4.(34) Sidgwick, N. W.; Sutton, L. E. *J. Chem. Soc. A* **1930**, 1461.(35) Lee, A. G. *J. Chem. Soc. A* **1971**, 2007.(36) Dahl, L. F.; Davis, G. L.; Wampler, D. L.; West, R. *J. Inorg. Nucl. Chem.* **1962**, *24*, 357.

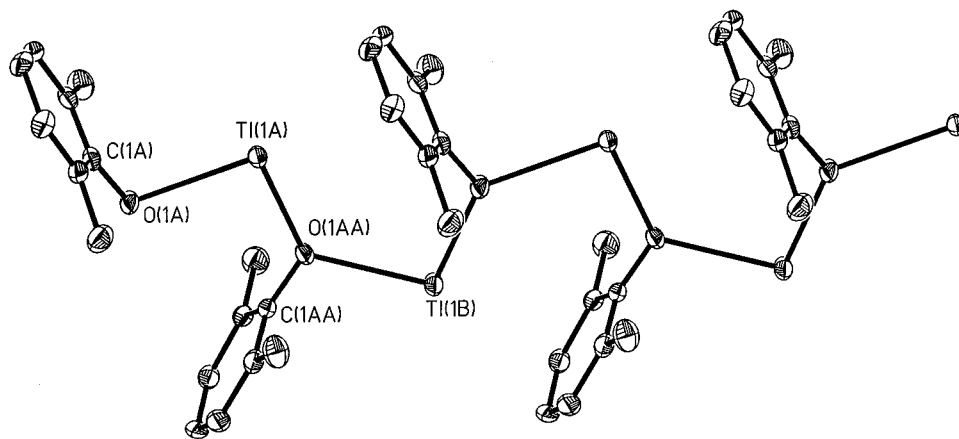


Figure 2. Thermal ellipsoid plot of **5**. Ellipsoids are drawn at 30% level.

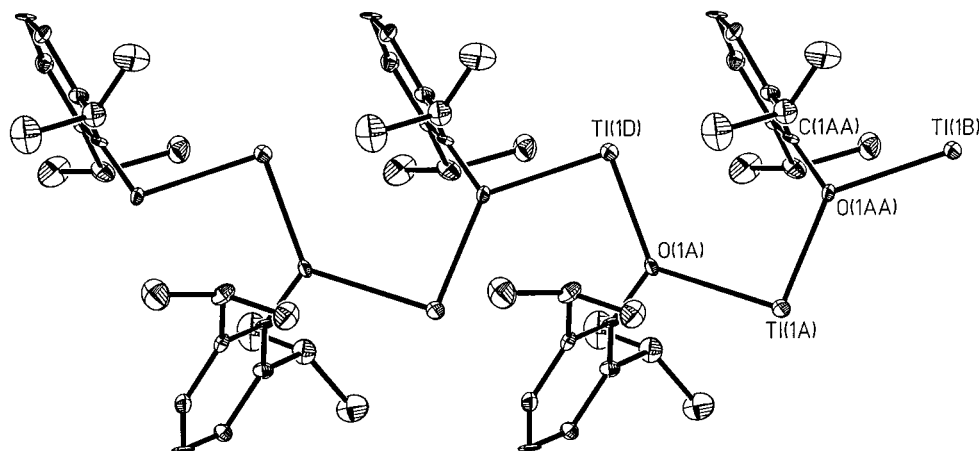


Figure 3. Thermal ellipsoid plot of **6**. Ellipsoids are drawn at 30% level.

hydrocarbon groups of the OCH_2CMe_3 ligands. The average Tl–O distance recorded for **4** were 2.47 Å. Because of the high symmetry of this molecule, the thermal factors are outside the normal range typically observed; however, the data collected are sufficiently reliable to be able to discuss the central core metrical data. In agreement with literature reports, the Tl atoms in **4** are formally three-coordinate, adopting a pyramidal geometry. The lone pair of electrons on each Tl metal center points outward, placing the Tl atoms in a distorted Td arrangement. The distortion of the cube observed in **4** was described by Dahl and co-workers as a cube containing superimposed Tl and O tetrahedra, with the oxygen tetrahedron being slightly smaller.³⁶ This distortion gives rise to Tl–O–Tl angles and O–Tl–O angles that are slightly greater and smaller than 90°, respectively. The Tl···Tl distance of the OMe³⁶ (3.84 Å) derivative is slightly longer than **4** (3.76 Å).

Figures 2 and 3 are the thermal ellipsoid plots of **5** and **6**, respectively. Both compounds, in contrast to the structurally identified $[\text{Tl}(\text{OR})_4]_n$ cubes, are one-dimensional polymers that possess a $[\text{Tl}-\text{O}]_n$ backbone (each backbone oxygen originating from an OAr ligand). For each compound, the Tl metal centers are two-coordinate, formally adopting a bent geometry; however, because of the presence of the lone pair on each metal center, metrical data consistent with a trigonal planar geometry were recorded. The Tl–O distances of **5** (av 2.48 Å) and **6** (av 2.51 Å) are statistically equivalent; however, there is one short (2.37 Å, **5**; 2.43 Å, **6**) and one long Tl–O distance (2.59 Å, **5**; 2.59 Å, **6**) recorded. The shorter metal–oxygen distance in each of the two species is concurrent with a larger Tl–O–C angle (**5**, 125.0° vs 103.8°; **6**, 124.6° vs 106.6°). Coupled with the

alternating short and long Tl–O distances, the chain incorporates alternating small and large angles (for **5**, O–Tl–O = 92.2°, Tl–O–Tl = 131.1°; for **6**, O–Tl–O = 92.8°, Tl–O–Tl = 128.1°). There are no discernible interactions between the polymeric strands of either **5** or **6**.

The bent polymeric chain structures observed for **5** and **6** are consistent with literature reports on other polymeric Tl species, such as the family of cyclopentadienyl (Cp) thallium ligated compounds, which includes $[\text{Tl}(\text{Cp})]_n$ ²⁸ and $[\text{Tl}(\text{Cp}^*)]_n$.²⁹ The structure of the $[\text{Tl}(\text{Cp})]_n$ complex was described as a “zigzag of equidistant metal atoms” (Tl···Tl···Tl = 100°). $[\text{Tl}(\text{Cp}^*)]_n$ also forms a polymeric zigzag chain structure (Tl···Tl···Tl = 146.4° av) but with shorter Tl···Tl distances (av 5.42 Å) representing a higher degree of covalent bonding.²⁹ In comparison, the Tl···Tl distances of **5** (av 4.52 Å) and **6** (4.51 Å) are statistically equivalent, as are the Tl···Tl···Tl angles (**5**, 94.5°; **6**, 94.0°). The bent nature of these chains is often associated with the stereochemically active lone pair of electrons present on each of the Tl atoms.^{14,37–40} An alternative explanation of the bent chains observed for **5** and **6** may involve the lack of s and p orbital mixing. This leads to M–L bonding that involves mainly the p orbitals with the lone pair of electrons residing in the s orbital. This argument, often referred to as the

(37) Ferguson, G.; Jennings, M. C.; Lalor, F. J.; Shanahan, C. *Acta Crystallogr.* **1991**, C47, 2079.

(38) Cowley, A. H.; Geerts, R. L.; Nunn, C. M.; Trofimenko, S. *J. Organomet. Chem.* **1989**, 365, 19.

(39) Mann, K. L. V.; Jeffery, J. C.; McCleverty, J. A.; Ward, M. D. *Polyhedron* **1999**, 18, 721.

(40) Bardwell, D. A.; Jeffery, J. C.; McCleverty, J. A.; Ward, M. D. *Inorg. Chim. Acta* **1998**, 267, 323.

“inert pair effect”, has been used to describe the bonding in a number of heavy metal main group complexes.^{41–44} Because of the rarity of nonstereochemically induced geometries observed for Tl(I) compounds,^{14,39,40} we reason that the lone pair of electrons on each Tl plays a significant role in determining the geometry of **5** and **6**; however, the degree of bending for the polymer chain will also be affected by the steric bulk of the OAr ligand.¹⁴

In contrast to **5** and **6**, the two previously reported [Ti(OAr)]₂ complexes, [Ti{μ-O(C₆H₄)(C₆H₄OH)}]₂³⁰ and [Ti(OC₆H₂-2,4,6-(CF₃)₃)]₂,³¹ were found to be dinuclear. The Tl metal centers in the dimers are supported by very different aromatic alcohols but inhabit nearly identical coordination environments. For each, the Tl atoms are bound to two bridging OAr ligands, thereby rendering the bonding analogous to that observed in **5** and **6**; hence, it is not readily apparent why **5** and **6** would prefer polymeric structures over discrete molecules.

Solution State. To determine if the solid-state structures of **4–6** were retained in solution, ¹H and ¹³C solution NMR experiments were undertaken. For each compound, both spectra revealed only a single set of resonances for each ligand set. Because of the high molecular symmetry of the solid-state structures of **4–6**, only a single set of peaks is expected for the intact species; however, dynamic solution behavior may also yield a similar spectrum. Fortunately, because of the natural occurrence of two spin-active Tl isotopes (²⁰³Tl and ²⁰⁵Tl) and their high sensitivity, Tl···Tl splitting could be used to elucidate solution structure where ¹H and ¹³C NMR spectroscopy investigations fail. ²⁰⁵Tl was one of the first nuclides investigated by NMR techniques because it is the third most receptive *I* = 1/2 nuclide.^{45,46} In principle, fine structure produced by Tl···Tl coupling can be very complex because both ²⁰⁵Tl and ²⁰³Tl are spin *I* = 1/2 nuclei with a natural abundance of 70.5% and 29.5%, respectively. Previous solution studies on [Ti(OR)]₄ concluded that the alkoxide species were tetrameric on the basis of the observed intensity ratios from Tl···Tl coupling in ²⁰⁵Tl NMR, even though only three of the expected seven lines were observed.¹⁸

Shown in Figure 4 are the observed spectra for the solution ²⁰³Tl NMR of **1–4**. The analogous spectra for the ²⁰⁵Tl NMR are shown in Figure 5. Figure 6 contains the simulated spectra and intensity ratios for ²⁰³Tl and ²⁰⁵Tl NMR of [Ti(OR)]₄ in which the splitting is the result of Tl···Tl scalar coupling in a species containing two, three, or four equivalent metal centers. Table 3 lists the observed and expected intensity ratios for the ²⁰³Tl NMR of compounds **1–4**. The observation of seven-line patterns verifies that the tetranuclear species isolated in the solid state (vide infra) must also be present in solution. This seven-line pattern is actually the superposition of a singlet (all one isotope—the resonating nuclide), doublet (one nonresonating nuclide), triplet (two nonresonating nuclides), and quartet (three nonresonating nuclides). Furthermore, since the observed intensity ratios are in good agreement with those expected for a tetranuclear species, it must be the major aggregate in solution. The observation of Tl···Tl coupling in **1–4** establishes an upper limit for fluxional processes that may be occurring ($\ll^2 J_{203-205} \approx 2.5$ kHz). In contrast, the ^{203,205}Tl NMR spectra of **5** and **6** reveal a singlet for each compound. The single ^{203,205}Tl

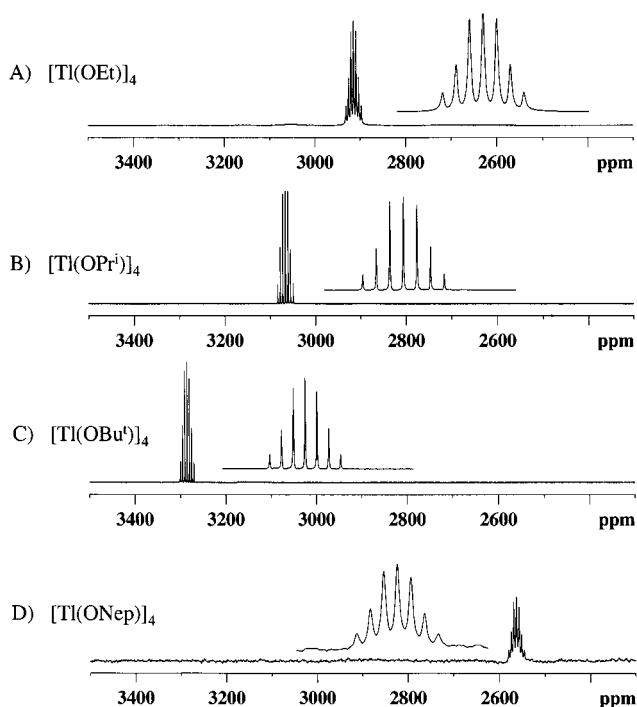


Figure 4. ²⁰³Tl solution NMR spectra (toluene-*d*₈) for (A) **1**, (B) **2**, (C) **3**, (D) **4**.

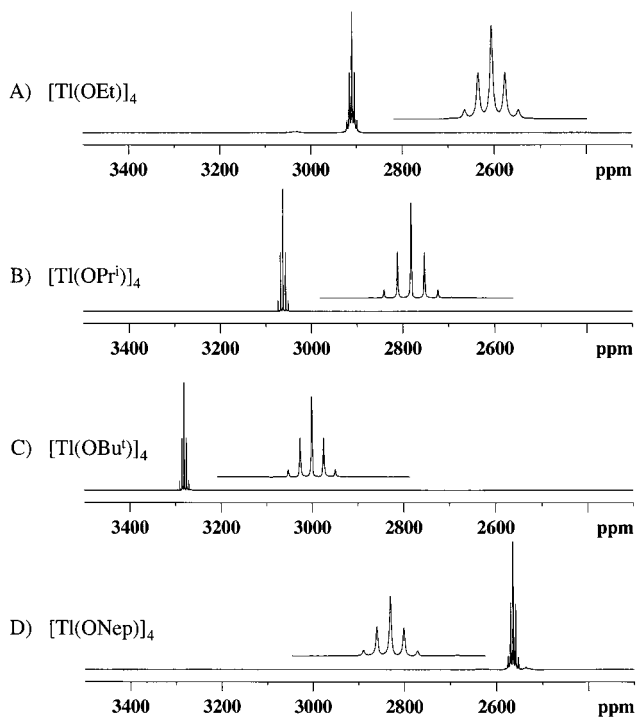


Figure 5. ²⁰⁵Tl solution NMR spectra (toluene-*d*₈) for (A) **1**, (B) **2**, (C) **3**, (D) **4**.

resonance is consistent with either the formation of a mono-metallic complex in solution or the presence of a fluxional process involving a dissociation/association equilibrium. In contrast to **1–4**, the lack of Tl···Tl coupling establishes a lower limit to possible fluxional processes ($\gg^2 J_{203-205} \approx 2.5$ kHz) in **5** and **6**.

As discussed previously, Lee indicated that a decrease in the *pK*_a of the parent alcohol results in an increase in the ionic character of the final “Ti(OAr)”.³⁵ The above observation was made for a series of aryl alcohols that had only covered a small

(41) ShimoniLivny, L.; Glusker, J. P.; Bock, C. W. *Inorg. Chem.* **1998**, *37*, 1853.

(42) Pyykko, P. *Chem. Rev.* **1988**, *88*, 563.

(43) Power, P. P. *Chem. Rev.* **1999**, *99*, 3463.

(44) Kaupp, M.; Schleyer, P. V. J. *Am. Chem. Soc.* **1993**, *115*, 1061.

(45) Hinton, J. F. *Magn. Reson. Chem.* **1987**, *25*, 659.

(46) Bloembergen, N.; Rowland, T. J. *Acta Metall.* **1953**, *1*, 731.

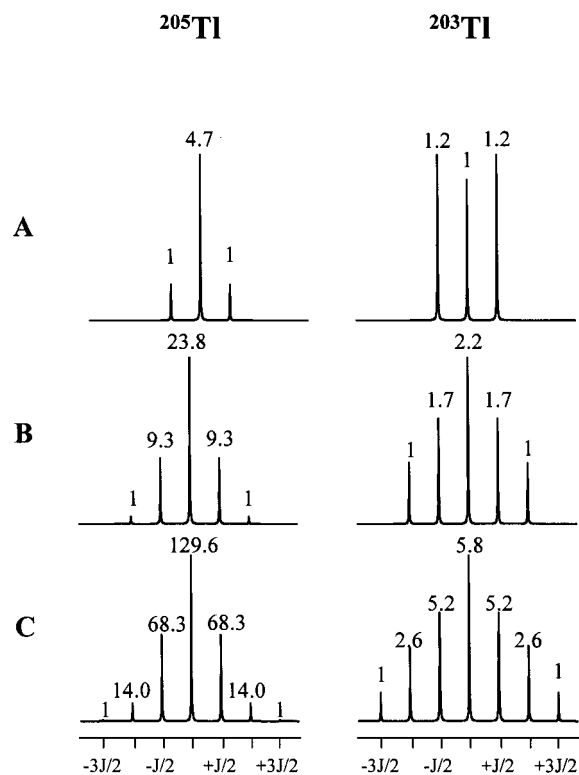


Figure 6. Simulated ^{205}Tl and ^{203}Tl NMR spectra for different sized Tl metal clusters as a function of the Tl–Tl scalar coupling: (A) a two Tl center cluster; (B) a three Tl center cluster; (C) a four Tl center cluster. The relative intensity ratio for the different multiplets is shown.

Table 3. Calculated and Observed Intensity Ratios for ^{205}Tl and ^{203}Tl NMR of Thallium Alkoxides

compound	septet intensity ratio						
	Calculated						
	1	2.6	5.2	5.8	5.2	2.6	1
	Observed						
1	1	2.7	5.4	6.0	5.4	2.7	1
2	1	2.9	5.9	6.0	5.9	2.9	1
3	1	2.8	5.7	6.4	5.7	2.8	1
4	1	2.7	6.0	6.8	6.0	2.7	1

$\text{p}K_{\text{a}}$ range. For **1–6**, the $\text{p}K_{\text{a}}$ of the parent alcohol significantly decreases as the ligand is changed from an alkoxide to an aryloxy. If the trend described by Lee is more general,³⁵ an increase in the ionic character will be observed going from **1** to **6**, which should result in a decrease in solubility in nonpolar solvents. As mentioned previously, the $[\text{Tl}(\text{OAr})_n]$ (**5** and **6**) are significantly less soluble in nonpolar solvents in comparison to **1–4**. Furthermore, an upfield shift of the corresponding $^{203,205}\text{Tl}$ resonances of $[\text{Tl}(\text{OAr})_\infty]$ in comparison to the $[\text{Tl}(\text{OR})_4]$ is observed and is expected for an increase in ionic character. Therefore, the $[\text{Tl}(\text{OAr})_\infty]$ complexes are more ionic than their $[\text{Tl}(\text{OR})_n]$ counterparts, and this difference can be observed in the $^{203,205}\text{Tl}$ chemical shift and predicted from the $\text{p}K_{\text{a}}$ of the parent alcohol.

This general chemical shift trend was also observed in the solid-state ^{205}Tl NMR of **2–6**. Table 4 contains the solution and solid-state ^{205}Tl chemical shift values of **1–6** and the $\text{p}K_{\text{a}}$'s^{47–49} of their corresponding alcohols. These data are presented graphically in Figure 7, and while there are minor

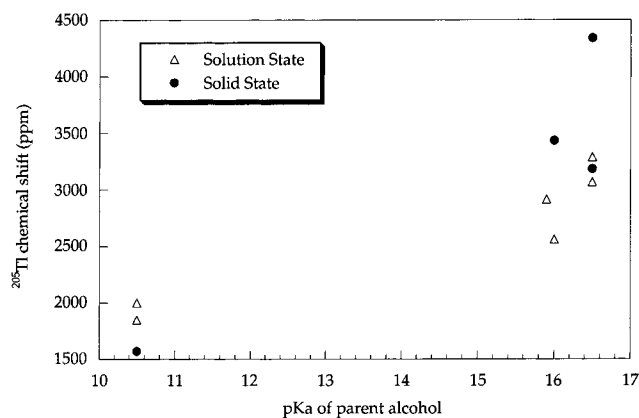


Figure 7. Graph of ^{205}Tl chemical shift vs $\text{p}K_{\text{a}}$ of the parent alcohol.

Table 4. Chemical Shift Values for ^{205}Tl NMR of **1–6** and $\text{p}K_{\text{a}}$'s of Corresponding Alcohols

compound	δ (ppm)		$\text{p}K_{\text{a}}$ of parent alcohol
	solution ($J_{203-205}$, kHz)	solid state	
1	2914 (2.54)		15.9 ⁴³
2	3067 (2.57)	3184	16.5 ⁴³
3	3287 (2.35)	4340	16.5 ⁴³
4	2561 (2.58)	3437	16 ⁴⁴
5	1999	3150, 2120, 1880	10–11 ⁴⁵
6	1850	1570	10–11 ⁴⁵

deviations, the general trend exists wherein an increase in ionic character results in an upfield chemical shift. This was observed for both the solid-state and solution-state $^{203,205}\text{Tl}$ NMR data. Chemical shift values for **5** are not included in Figure 7 because they were ambiguous, and experiments to clarify these results are underway. There was one predominant resonance observed in the spectrum of **5** with several minor resonances also noted. The minor resonances of **5** in the solid-state NMR spectrum may be a reflection of intramolecular $\text{Tl}\cdots\text{Tl}$ packing interactions or minor impurities. The minor impurities are unlikely because the elemental analysis and the solution-state $^{203,205}\text{Tl}$ NMR data indicate the presence of one only compound. The minor Tl resonances are not observed for the solid-state NMR spectrum of **6**.

The dependence of the ^{205}Tl chemical shift on both solvent and concentration has been reported for numerous Tl(I) complexes.^{45,50,51} This characteristic has even been exploited as a means of establishing solvent donor numbers.^{52,53} The Tl chemical shift dependence upon concentration is generally less significant, as evidenced by an order of magnitude variation in concentrations for both **1** and **5**, which resulted in only slight chemical shift differences (<20 ppm). For the cubane structure of **4**, the seven-line ^{203}Tl resonance was found to exist independently of the solvent utilized for dissolution and was observed at very similar frequencies (<20 ppm difference). This indicates that the Tl cations of the cubane structures are almost completely protected from outside influences (i.e., no coordination of solvent is possible for the cubane structure).

In the case of **5**, a chemical shift difference was observed when the compound was dissolved in solvents of differing donor

(47) Reeve, W.; Erikson, C. M.; Aluotto, P. F. *Can. J. Chem.* **1979**, *57*, 2747.

(48) Takahashi, S.; Cohen, L. A.; Miller, H. K.; Peake, E. G. *J. Org. Chem.* **1971**, *36*, 1205.

(49) Bordwell, F. G.; McCallum, R. J.; Olmstead, W. N. *J. Org. Chem.* **1984**, *49*, 1424.

(50) Srivanavit, C.; Zink, J. I.; Dechter, J. J. *J. Am. Chem. Soc.* **1977**, *99*, 5876.

(51) Siddique, R. M.; Winfield, J. M. *J. Fluorine Chem.* **1988**, *40*, 71.

(52) Briggs, R. W.; Hinton, J. F. *J. Solution Chem.* **1977**, *6*, 827.

(53) Briggs, R. W.; Hinton, J. F. *J. Solution Chem.* **1979**, *8*, 519.

ability, δ 1989 in toluene and δ 1916 in pyridine. Independent of the counterion, the ^{205}Tl resonance for dilute $\text{Tl}(\text{NO}_3)_n$ in pyridine appears at ~ 800 ppm.⁵² The upfield shift for the pyridine sample of **5** (toward 500 ppm) would be expected if any solvent/metal interactions were present. The slight change noted above indicates that the Tl^+ in **5** can interact with strong Lewis basic solvents, but this does not occur to a great extent. Furthermore, exposure of **5** and **6** to strong Lewis basic solvents during crystallization did not result in any metal/solvent interactions observed in the solid-state structures. The larger solvent dependence on chemical shift and increased solubility in polar solvents also supports the view of $[\text{Tl}(\text{OAr})_n]$ as generally more ionic in comparison to their alkyl counterparts (vide infra). The dissociation/association equilibria expected for ionic species may also explain the absence of $\text{Tl}\cdots\text{Tl}$ coupling in the NMR spectra of **5** and **6**.

Summary and Conclusion

We have successfully synthesized and characterized a series of $[\text{Tl}(\text{OR})_n]$ compounds. While the simple alkoxides adopt a cubane structure ($n = 4$; **1–4**), the bulky aryloxides form novel one-dimensional $[\text{Tl}(\text{OAr})_n]$ polymers ($n = \infty$; **5** and **6**). The ^{205}Tl MAS NMR spectra obtained on these compounds were consistent with the solid-state structures except for **5**, which displayed multiple minor resonances. $^{203,205}\text{Tl}$ solution NMR of **1–4** confirmed that these samples maintained their cubane

structures in solution, consistent with literature reports, and were unaffected by the choice of solvent. In contrast, the more ionic species **5** and likely **6** display increased solvent dependence on chemical shift. Chemical shift values from the $^{203,205}\text{Tl}$ solution NMR of **1–6** follow a general trend wherein an increase in the metal ionic character correlates to a upfield shift. The degree of ionic character can be predicted, and increased covalency of the $[\text{Tl}(\text{OR})_n]$ complex can be imposed by utilizing stronger electron-donating alkoxides (increased $\text{p}K_a$ of the parent alcohol).

Acknowledgment. For support of this research, the authors thank the United States Department of Energy for Contract DE-AC04-94AL85000. Sandia is a multiprogram laboratory operated by Sandia Corporation, a Lockheed Martin Company, for the United States Department of Energy. The authors thank Karen Ann Smith for continued access to the ASX300 spectrometer and Martine Ziliox for loan of the solid-state Tl preamplifier.

Supporting Information Available: Full summaries of X-ray diffraction data, listings of atomic coordinates and anisotropic thermal parameters, hydrogen atom positions, and full bond distances and angles. This material is available free of charge via the Internet at <http://pubs.acs.org>.

IC0006192